Clay Minerals, (2015) **50**, 297–306

Crystal chemistry of Na-rich rectorite from North Little Rock, Arkansas

JAN DIETEL[1,*], ANNETT STEUDEL[2], LAURENCE N. WARR[1] AND KATJA EMMERICH[2]

[1] *Institute of Geography and Geology, Ernst-Moritz-Arndt University Greifswald, 17487, Greifswald, Germany*
[2] *Competence Center for Material Moisture (CMM) and Institute for Functional Interfaces (IFG), Karlsruhe Institute of Technology, Hermann-von-Helmholtz-Platz 1, D-76344 Eggenstein-Leopoldshafen, Germany*

(*Received 3 December 2014; accepted 10 April 2015; Associate Editor: H. Stanjek*)

ABSTRACT: The rectorite, a regular mixed layer mineral consisting of dioctahedral swelling and non-swelling 2:1 layers, from North Little Rock, Arkansas, was studied to define the crystal chemistry and structural parameters (e.g. layer charge of the different layers, presence of *cis*/*trans*-vacancies). X-ray diffraction, simultaneous thermal analysis coupled with mass spectrometry, X-ray fluorescence and cation exchange capacity are used to characterize this rectorite. The rectorite has a coefficient of variation (CV) of 0.19 and a cation exchange capacity of 60 cmol(+)/kg, as determined by the ammonium acetate method. The mineral is best described as a regular interstratification of brammallite-like and high-charged beidellite-like layers. Dehydration occurs at ≈118°C with a mass loss of 6.77% and dehydroxylation occurs in two steps at 470°C and 588°C with an overall mass loss of 4.67%. Peak decomposition of the mass spectrometer curve of evolved water shows ≈20% peak area with a maximum higher than 600°C, indicating ≈20% *cis*-vacant layers.

KEYWORDS: rectorite, regular interstratification, crystal chemistry, simultaneous thermal analysis, *cis*/*trans*-vacancy.

Rectorite, previously known as allevardite, is defined as a regular, interstratified 2:1 layer silicate, composed of dioctahedral mica with dioctahedral smectite (Caillère & Henin, 1950). The prefixes Na-rich, K-rich or Ca-rich describe the dominant cation present in the mica interlayer (Bailey, 1982; Guggenheim *et al*., 2006). Well-crystallized rectorite occurs in hydrothermal veins (<350°C) exposed in Jeffrey Quarry, Arkansas, where clay alteration zones occur. Rectorite has also been described in altered bentonites and as an alteration product of muscovite during shale diagenesis (Anthony *et al.*, 1995). There are 11 reported locations of rectorite in Arkansas (Miser & Milton, 1964) with a further approximately eight localities worldwide (e.g. Kitagawa, 1997; Matsuda *et al*., 1997). This rare mineral is considered suitable for the formulation of chitosan/organic rectorite nanocomposite films that have promising applications as carriers for drug delivery or antimicrobial agents (Wang *et al*., 2006).

Bradley (1950) and Miser & Milton (1964) described Na-rich rectorite from Arkansas as an interstratification of pyrophyllite and vermiculite or montmorillonite. In contrast, Brown & Weir (1963), Barron *et al*. (1985a,b), Klimentidis & Mackinnon (1986) and Jakobsen *et al*. (1995) considered the non-swelling 2:1 layers of rectorite from Arkansas to be micaceous instead of pyrophyllitic. Using solid-state NMR, Jakobsen *et al*. (1995) considered that the micaceous 2:1 layers belong to paragonite with significant Al tetrahedral substitution. Studies of rectorite from other locations also described rectorite as an interstratified mineral with mica-like and smectite-like layers, but without identifying the mica or smectite type (Brown & Weir, 1963), or by considering the smectite as montmorillonite (Gradusov *et al.*, 1968). Jakobsen *et al*. (1995) and Kodama (1966) described a rectorite from Pakistan as being an ordered mixed-layer phase consisting of non-swelling paragonite-like layers and swelling beidellitic and montmorillonitic layers.

* E-mail: jandietel@gmx.de
DOI: 10.1180/claymin.2015.050.3.04

In this study, the crystallographic and chemical characteristics of the rectorite from North Little Rock, Arkansas were analysed in detail by transmission electron microscopy (TEM), X-ray diffraction (XRD), simultaneous thermal analysis (STA), X-ray fluorescence (XRF) and Cu-triene and ammonium acetate cation exchange methods. Based on relatively pure separates, improved constraints are presented for identifying the layer components and charge distributions that comprise the ordered interstratified structure and the nature of the *trans*- (*tv*) and *cis*- (*cv*) vacancies in this rectorite.

MATERIALS AND ANALYTICAL METHODS

Starting material

Rectorite from the Jeffrey Quarry occurs in veins and fissures in the Mississippian Jackfork Sandstone where it is associated with dispersed quartz crystals, cookeite aggregates, sulfides (pyrite, sphalerite, galena), carbonates and rutile. Rectorite forms a gel-like material with high viscosity owing to sorption of water. On drying, the gelatinous material forms yellowish flexible flakes of rectorite (Miser & Milton, 1964).

The Jeffrey Quarry rectorite studied was obtained from the Ernst-Moritz-Arndt-University Greifswald clay mineral collection. The sample consists of soft aggregates of rectorite and cookeite foliae together with quartz crystals in accordance with the descriptions of Brown & Weir (1963) and Miser & Milton (1964). Rectorite was separated by disaggregating the sample with ultrasound in deionized water and centrifugation at 4000 rpm and 20°C for 79 min to obtain the <0.1 μm fraction (Eppendorf Centrifuge model 5810 R).

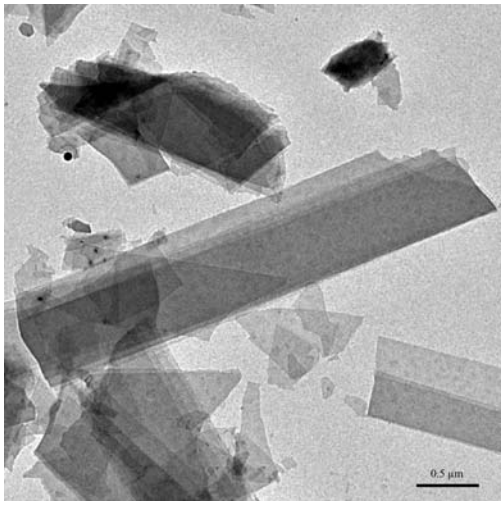

FIG. 1. TEM image of the Arkansas rectorite showing typical laths and fragments that overlie each other partially. The small black spots (left side of image) are unknown particles.

Methods

The morphological description of the mineral particles was undertaken using a Jeol JEM 1210 transmission electron microscope. The samples were dispersed by ultrasonic treatment in distilled water and sedimented on C-coated Cu-grids. Images were obtained at magnifications between 1000x and 3000x with an accelerating voltage of 120 kV.

The XRD analysis was carried out with a Bruker D8 Advance θ–θ diffractometer using Fe-filtered CoKα radiation generated at 40 kV and 30 mA. The diffractometer was equipped with a 0.5° divergence slit, an 8 mm antiscatter slit and a 1D LynxEye detector that includes 14 strips each with a height of 0.075 mm. A step size of 0.02°2θ was used and scans were made between 3 and 100°2θ (scan rate 2.4 s/step) for randomly oriented powders and 2.5–80°2θ (scan rate 0.4 s/step) for preferred oriented samples (surface density of ≈4 mg/cm^2). The oriented samples were examined in the air-dried state, after ethylene glycol-saturation and after heating at 550°C. The coefficient of variation (CV), which describes the regularity of alternation of an interstratification, was calculated from the ethylene glycol-saturated sample pattern. A CV of <0.75 is one requirement to allocate a mineral name, such as rectorite or corrensite, to a regularly interstratified phase (Bailey, 1982; Guggenheim *et al*., 2006).

At least three orders of basal reflections, including two odd orders, must be observed and at least ten (00*l*) values must be obtained (Bailey, 1982; Guggenheim *et al*., 2006), with similar peak breadths (full width at half maximum, FWHM). The CV was calculated according to Bailey (1982). The FWHM parameter was determined using the method described by Kübler (1964, 1967) after stripping Kα$_2$ and correcting for angular-dependent broadening.

Major-element chemical analyses were obtained with a Philips PW 2404 XRF spectrometer equipped with a Philips PW 2540 vrc sample changer. The sample was heated at 105°C (20 h) and then calcined at 1050°C (1 h) to determine the loss on ignition (LOI). A

fusion bead was obtained after melting the sample with a flux ($LiBO_2 + Li_2B_4O_7$) at ≈1100°C.

The chemical analyses were used to calculate the structural formula following Stevens (1946). The cation exchange capacity (CEC) was measured with 0.01 M Cu-triethylenetetramine (Cu-triene) (Meier & Kahr, 1999; Steudel *et al*., 2009; Wolters *et al*., 2009). The ammonium acetate CEC method (Schollenberger & Dreibelbis, 1930; Mackenzie, 1951) was used for high-charged layers because the Cu-triene method often yields values that are too low (Steudel *et al*., 2009). The exchangeable cations were analysed subsequently by inductively coupled plasma optical-emission spectroscopy (ICP-OES, Optima 8300 DV Perkin Elmer). The sum of the individual exchangeable cations coincided well with the CEC values. A detailed description of this method has been given by Steudel & Emmerich (2013).

Simultaneous thermal analysis coupled with mass spectrometry (STA-MS) measurements were performed using an STA 449 C Jupiter thermal analyser (NETZSCH-Gerätebau GmbH) equipped with a thermogravimetry/differential scanning calorimetry sample holder. The STA was connected to a quadrupole mass spectrometer 403 C Aëolos (InProcess Instruments 10 (IPI)/Netzsch-Gerätebau GmbH). The measurements were made in the temperature range 35–1100°C, at a heating rate of 10°C/min under a synthetic air/nitrogen (SA, 50 mL/min; N_2 20 mL/min) mixed atmosphere. Conventional Pt/Rh crucibles with lids (diameter = 5 mm and height = 5 mm) were used and an empty crucible was measured as a reference. Prior to the dynamic segment, the sample was exposed to the dry gas atmosphere at 35°C for 15 min. The mass loss due to dehydration was then calculated from the mass loss in both segments. All subsequent mass losses were normalized to the dry weight after dehydration for stoichiometric analysis. Although classification of dioctahedral smectites and interlayer deficient micas (Wolters & Emmerich, 2007) are based on sample weights of 100 mg, only 43 mg were used without compaction owing to the low bulk density of the rectorite powder. Hence, recording sample-amount dependency curves (so-called PA-curves, after Smykatz-Kloss, 1967) was necessary. The PA-curves may display shifts of the maximum peak temperature during mineral decomposition owing to the sample weight or to the different concentration of the mineral in any given mixture (Smykatz-Kloss, 1967). For terms of reference, the PA-curves of a mainly *trans*-vacant Fe-rich smectite (Valdol, Wolters & Emmerich, 2007), a predominant *trans*-vacant illite (Arginotec NX), a mainly *cis*-vacant smectite (Bentonite P) and a *cis*-vacant smectite (Volclay, Wolters & Emmerich, 2007) were measured using sample weights ranging between 5 and 100 mg. These results were used to determine the temperature of the peak maxima in the STA curves of the rectorite.

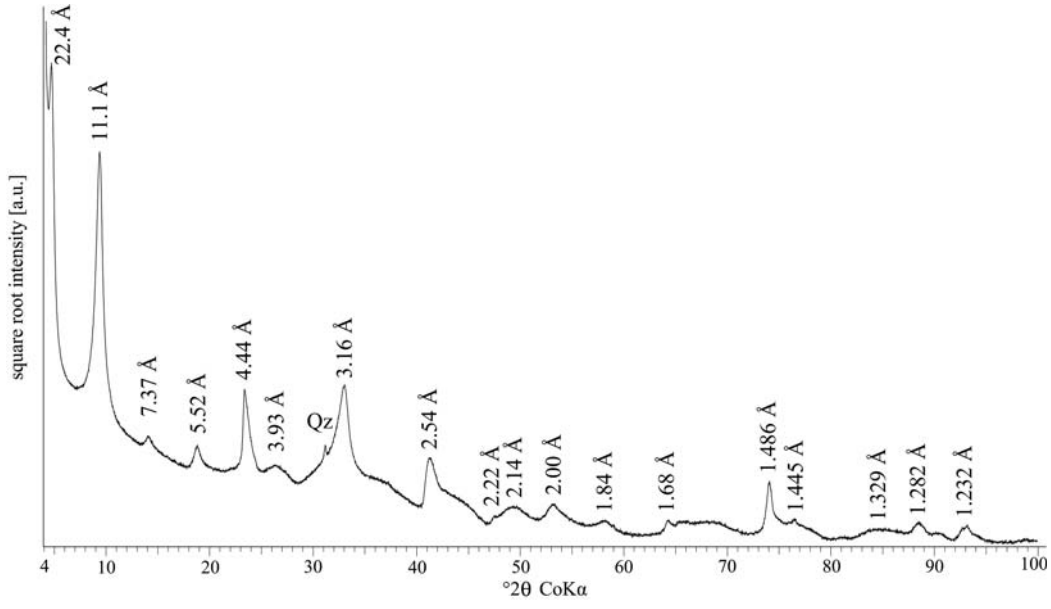

FIG. 2. Random powder XRD pattern of the rectorite <0.1 μm fraction containing a small amount of quartz. The *d* spacings given refer to rectorite.

The *cis*- and *trans*-vacant character of the octahedral sheet was determined by peak decomposition of the mass spectrometer curve of evolved water (m/z = 18) in the range 350–900°C using *PeakFit* (Version 4.12; SeaSolve Software, Framingham, Massachusetts, USA). The relative areas of all peaks with maxima of <600°C and >600°C were summed and the ratio of both areas taken to reflect the number of *trans*- and *cis*-vacant octahedral sheets (Drits *et al*., 1998; Wolters & Emmerich, 2007; Wolters *et al*., 2009).

RESULTS AND DISCUSSION

Micromorphology

Examination by TEM showed thin elongated laths of rectorite, partially overlying each other (Fig. 1). Some of the lath plates are kinked, folded or broken. These observations are similar to the particle shapes described for rectorite from Allevard (Kitagawa, 1997; Brown & Weir, 1963), Dagestan, Baluchistan and Arkansas (Brown & Weir, 1963) and for illite-smectite (I-S) interstratifications with about 50% expandable layers (Inoue 1987, 1988). Some particles showed dark spots with a diameter between 65 and 125 nm, which were too small for compositional determination.

Purity and chemical composition

The random powder XRD pattern showed that the <0.1 μm fraction consisted of dioctahedral rectorite (>98 mass%), ≈0.6 mass% quartz (Fig. 2) and minor amounts of cookeite (<1 mass%); the latter was detected only in preferred-orientation mounts (Fig. 3). In addition, the organic content was determined by STA measurements, as were traces of barite and Sr-rich carbonate and/or Sr-rich sulfate, marked by the release of CO_2 or SO_2, respectively (data not shown).

The CV value of 0.19 with similar FWHM values between 0.28°2θ and 0.46°2θ confirms the regular interstratified 2:1 layer silicate as rectorite (Fig. 4). The XRF results indicate very low Mg, Ca, K, Ba, Sr and structural Fe content (Table 1). Ba and Sr were not included in the structural formula owing to their low abundances. Based on its composition, this rectorite was classified as Na-rich, as the high Na_2O content (4.53 mass%) indicates that this cation dominates both the interlayers of the mica layers (paragonite or the so-called brammallite, which is a Na-rich interlayer-deficient dioctahedral mica that has not been approved as a mineral by the International Mineralogical Association) and the swelling smectitic layers.

The traces of quartz, detected by XRD, were subtracted from the compositional analyses and the results were normalized to the dry state. The TiO_2, MnO and ZnO contents were between 0.01 and 0.09 mass%. As these cations are not known to participate in the rectorite structure, they were excluded from the structural formula calculations.

Intercalation of NH_4^+ cations resulted in a greater CEC value than intercalation of Cu-triene (Table 2), the latter probably reflecting incomplete intercalation

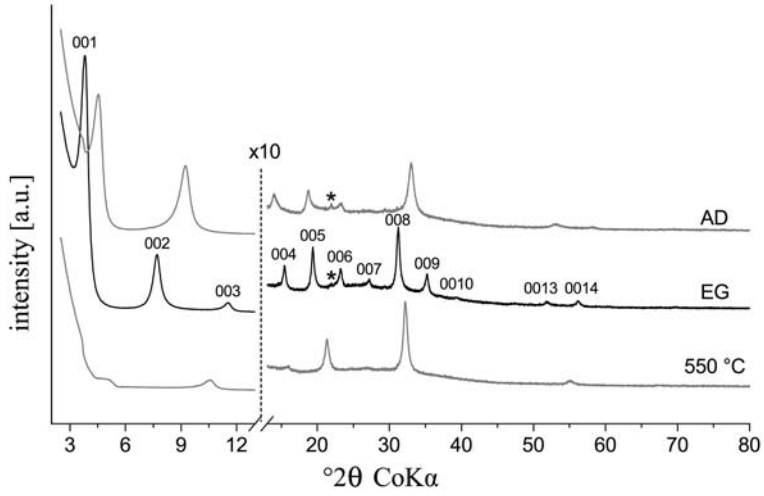

FIG. 3. XRD pattern of the oriented <0.1 μm fraction rectorite sample, air dried (AD), ethylene glycol saturated (EG) and heated at 550°C. * = trace impurity of cookeite.

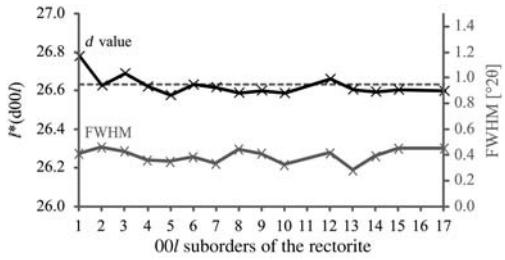

FIG. 4. Measured *d* values (black) and their mean (dashed line) used for CV-value determination of rectorite from North Little Rock, Arkansas. The CV values were determined from the XRD pattern of an EG-saturated, oriented sample. FWHM: Full width half maximum (grey).

in the presence of divalent cations in high-charge smectitic layers (Steudel *et al*., 2009).

The structural formula of the rectorite was determined as follows:

$$(Na_{0.53}Mg_{0.03}Ca_{0.03}K_{0.02})$$
$$(Al_{1.96}Fe^{3+}_{0.05}Mg_{0.02})\ [(Si_{3.26}Al_{0.74})\ O_{10}(OH)_2] \quad (1)$$

The layer charges of –0.74 mol(+)/mol F.U. for tetrahedral sheets and +0.06 mol(+)/mol F.U. for octahedral sheets are similar to values calculated by Brown & Weir (1963), Kodama (1966) and Jakobsen *et al*. (1995). A slightly positive octahedral charge is indicated (Table 3), although Miser & Milton (1964) did not calculate octahedral charge. If all divalent interlayer cations are allocated to the smectitic layers as indicated by CEC measurements and ICP-OES data of exchanged cations, the average composition of the smectitic layers is:

$$(Na_{0.24}Mg_{0.06}Ca_{0.06})$$
$$(Al_{1.93}Fe^{3+}_{0.11}Mg_{0.02})[(Si_{3.36}Al_{0.64})O_{10}(OH)_2] \quad (2)$$

Thus, the non-swelling layers have an average composition of:

$$(Na_{0.81}K_{0.03})\ Al_{2.00}\ [(Si_{3.16}Al_{0.84})O_{10}(OH)_2]. \quad (3)$$

Hence the negative layer charges of both layer types are equivalent to 0.48 mol(+)/mol F.U. for the smectitic layers and 0.84 mol(+)/mol F.U. for the non-swelling layers, respectively. As most of the charge is located in the tetrahedral sheet, the smectitic layer approximates beidellite. As smectite is defined as lying between 0.2 mol(+)/mol F.U. (low charge) and 0.6 mol(+)/mol F.U. (high charge) (Guggenheim *et al*., 2006; Emmerich *et al*., 2009), the value determined denotes a high-charge smectitic layer. The non-swelling layers resemble interlayer deficient brammallite layers

TABLE 1. XRF chemical analyses of rectorite. Values [%] were normalized to ignited mass due to variable amounts of expandable smectitic layers. The LOI was 11.46 mass% (dehydration and dehydroxylation).

Reference	Present work	Miser & Milton (1964)	Kodama (1966)	Brindley (1956)
Locality	North Little Rock, Arkansas	North Little Rock, Arkansas	Baluchistan, Pakistan	Allevard, France
Element oxide	mass%			
SiO_2	54.60	54.69	53.98	54.29
Al_2O_3	38.38	39.20	40.28	38.62
Fe_2O_3	1.22	0.02	0.15	0.78
FeO	–	–	–	0.66
MgO	0.48	0.60	0.78	0.42
CaO	0.44	1.28	0.52	1.20
Na_2O	4.53	4.07	3.86	2.70
K_2O	0.20	0.14	0.29	1.32
BaO	0.08	–	–	–
SrO	0.06	–	0.13	–
Sum	99.99	100.00	99.99	99.99

Table 2. CEC values of rectorite from North Little Rock, Arkansas determined by the ammonium acetate (NH_4-Ac) and copper-triethylenetetramine (Cu-triene) methods. The CEC was determined in duplicate and the mean values were used for calculations.

	Intercalation complex	CEC [cmol(+)/kg]	Ø CEC [cmol(+)/kg]	Proportion of exchangeable cations [mmol/g]			
				Na	Mg	Ca	K
(1)	NH_4-Ac	60.2	60	0.44	0.08	0.04	0.00
	NH_4-Ac	60.6					
(2)	Cu-triene	50.2	50	0.48	0.05	0.02	0.00
	Cu-triene	49.8					

instead of ideal mica layers (paragonite-like), consistent with the definition of Rieder *et al*. (1998) and Guggenheim *et al*. (2006), where brammallite has a layer charge between 0.6 mol(+)/mol F.U. and 0.85 mol(+)/mol F.U. Similar small layer charges are observed in K-dominated compositions that are composed of illitic rather than muscovitic layers.

The determination of the structural formula presented contains uncertainties that may result in small errors. A major assumption for structural calculations is an ideal anionic network. Fe is assumed to be Fe^{3+} in the XRF results as the samples were melted and oxidized during sample preparation. However, the oxidation state of Fe for the untreated <0.1 μm fraction was not determined, but this should lead to few errors as Bishop *et al*. (2011) showed that <12% of the total Fe present is in the Fe^{2+} state for the Arkansas rectorite. In contrast, the rectorite from Allevard, France contains 0.45 mass% Fe^{3+} and 0.43 mass% Fe^{2+} (Brindley, 1956) and the greater Fe^{2+} content would result in a lower positive octahedral charge.

The XRF results yielded a slightly higher Mg content than the ICP-OES data from the CEC measurements. Some Mg is assumed to reside in the octahedral sites in addition to the interlayer. The structural formula determined indicated that <0.01 mol/mol F.U. of Mg resides in the octahedral sheet. To verify the structural formula, the calculation of the CEC was undertaken as follows:

$$\mathrm{CEC} = \frac{\xi}{M} * 100000 \qquad (4)$$

Where: ξ = layer charge of the smectitic layers [mol (+)/mol] and M = Molar mass [g/mol]. As only the smectitic layers are assumed to contain exchangeable cations, the layer charge of the smectitic layers was used for CEC calculations. Two formula units of

Table 3. Comparison of results with published data for the charge distribution in the tetrahedral and octahedral sheets and the interlayer of the rectorite (mol(+)/mol per 2 F.U.). The charges of the proposed beidellite and brammallite layers are given (mol(+)/mol per 1 F.U. each).

Reference	Phase	Charges [mol(+)/mol]		
		Tetrahedral	Octahedral	Interlayer
Present work	Beidellitic layer (1 F.U.)	–0.64	+0.16	+0.48
	Brammallitic layer (1 F.U.)	–0.84	0.00	+0.84
	Rectorite (2 F.U.)	–1.48	+0.16	+1.32
Brown & Weir (1963)	Rectorite (2 F.U.)	–1.32	+0.12	+1.20
Miser & Milton (1964)	Rectorite (2 F.U.)	–1.50	0.00	+1.50
Kodama (1966)	Rectorite (2 F.U.)	–1.58	+0.24	+1.34
Jakobsen *et al.* (1995)	Rectorite (2 F.U.)	–1.48	+0.22	+1.26

rectorite were used in the calculation.

$$\xi_{\text{smectitic layers}} = 0.48\ \frac{\text{mol}(+)}{\text{mol}}\ \text{per F.U.} \quad (5)$$

$$M_{\text{Rectorite}} = 376.37\ \text{g/mol} \quad (6)$$

$$\text{CEC}_{\text{Rectorite}} = \frac{0.48\text{mol}(+)/\text{mol}}{752.73\text{g/mol}} * 100000 = 64\ \frac{\text{cmol}(+)}{\text{kg}} \quad (7)$$

The structural formula calculated according to Stevens (1946) without measuring layer charge will overestimate the layer charge of swelling 2:1 layer silicates (Lagaly & Weiss, 1971) and, consequently, the CEC (Wolters *et al*., 2009, Kaufhold *et al*., 2011).

Based on the compositional constraints presented, the rectorite from North Little Rock, Arkansas, is best described as a regularly interstratified phase consisting of brammallitic and beidellitic layers. This interpretation is consistent with that of Brown & Weir (1963) who proposed brammallitic layers and interlayer-deficient mica layers. These results are generally consistent with the nature of illitic interstratifications (Środoń, 2013). However, they are at odds with Kodama (1966) and Jakobsen *et al*. (1995) who considered the Na-rich mica to be either paragonite-like or paragonite *sensu stricto*. In addition, the calculated layer charge of paragonite with its large degree of substitution, as proposed by Jakobsen *et al*. (1995), is not supported by other studies (e.g. Ahn *et al.*, 1985; Comodi & Zanazzi, 1997, 2000). Because the layer charge of the mica-like layers lies close to the phase boundary defined between paragonite and brammallite (0.85 mol(+)/mol F.U., Rieder *et al.*, 1998, Guggenheim *et al*., 2006), the different mica compositions may reflect sample heterogeneity in the materials studied or analytical errors.

The dehydration behaviour of rectorite in the differential scanning calorimetry (DSC) and mass spectroscopy (MS) curves of evolved water, with a peak maximum at 117 ± 2°C, is characteristic of expandable clay minerals with monovalent interlayer cations (in this case Na) stored at 20–25°C and a relative humidity (RH) of about 35–45%. The mass loss of 6.77% indicates <100% swelling layers (Fig. 5; Emmerich *et al.*, 2015) and the water loss at 105°C (H_2O) determined by oven heating was also 6.77 mass %, whereas the LOI of the dehydrated sample was 4.69 mass%. Both values are equal to the STA measurements and consistent with Kodama (1966), whereas Brindley (1956) determined a LOI value of 6.04 mass% related to the dry weight, which may reflect a larger organic content.

The traces of organic molecules detected did not appear to result from contamination during sample processing as oxidized organics were detected by a small exothermic peak (0.93 mass%) at 315°C in the DSC curve (Fig. 5), which was shown to be a release of water (m/z = 18) (Fig. 5, lower) and CO_2 molecules (m/z = 44, data not shown) by the MS curves (Fig. 5 middle). As the organic matter is scarce and there is no evidence of its intercalation in the interlayer from the measured *d* values determined by XRD, the organic molecules have a negligible effect on the structural formula. The organic matter is oxidized by heating during STA measurements prior to dehydroxylation of the rectorite and, hence does not affect the *trans*/*cis*-vacancy determination.

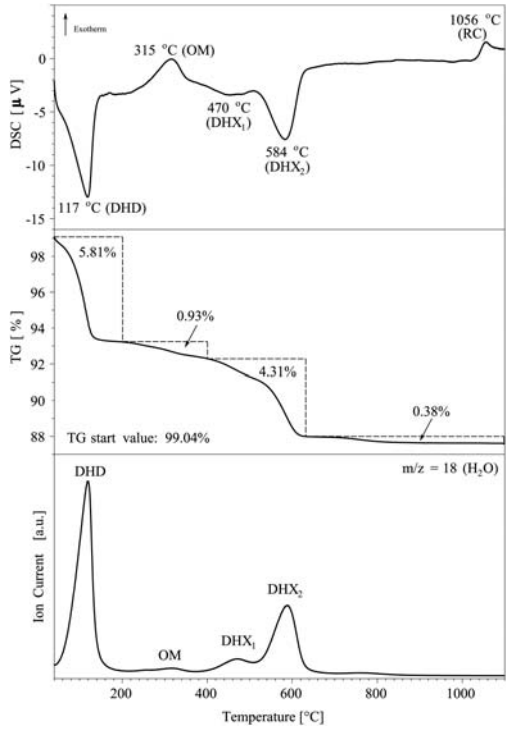

FIG. 5. STA-MS data for the <0.1 µm fraction of rectorite from North Little Rock, Arkansas. From top to bottom: DSC curve, TG curve (mass loss related to the starting sample weight, for values to the dry weight see text) and MS curve of evolved water. DHD: Dehydration, OM: Organic matter, DHX: Dehydroxylation, RC: Recrystallization.

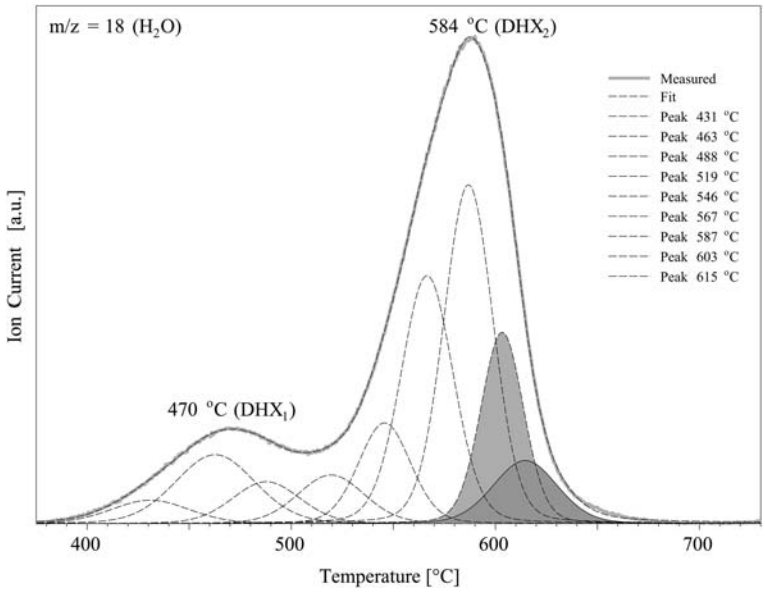

FIG. 6. Deconvolution of the MS curve of evolved water during dehydroxylation. Grey areas represent curves with peak maxima above 600°C that represent the number of *cv*-containing layers.

Dehydroxylation behaviour and trans-/cis-vacancy

Dehydroxylation occurred in two steps with peak maxima at 470°C and 584°C (± 3°C). The mass loss on ignition was 4.67 mass% and this value is less than the stoichiometric value of 4.78 mass%. The deviation is probably due to the uncertainty in determining the onset of dehydroxylation owing to the contemporaneous oxidation of organic material.

TDecomposition of the MS dehydroxylation-related curve revealed an ≈80% peak area below 600°C, which is believed to correspond to *tv* layers in rectorite (Drits *et al*., 1995) and ≈20% above 600°C that is attributable to *cv* layers (Fig. 6). The decomposition was modelled by using the smallest number possible of symmetrical peaks to obtain the best fit.

he slope of the PA-curves obtained from STA analysis in a log plot (data not shown) decreased with decreasing iron content. Because of the small Fe content of the rectorite, extrapolation of the maximum peak temperature for the second dehydroxylation peak of rectorite with a sample weight of 100 mg results in a temperature of ≈600°C and no shift of the *tv*/*cv* ratio occurs. The ratio of *tv* and *cv* layers determined from peak decomposition seems plausible for a regular interstratification of brammallite and beidellite. Assuming beidellitic layers are mainly *tv* (Tsipursky & Drits, 1984; Lantenois *et al*., 2008), the brammallitic layers should contain both *tv* and *cv* sites in the octahedral sheet. In accordance with this work, *cv* layers have been reported to predominate in what are usually, *tv*-dominated illites and illite fundamental particles within I-S interstratifications containing more than 1.55 and 0.35 Al atoms per F.U. in the octahedral and tetrahedral sheets, respectively (Drits & Zviagina, 2009). Because these data fit well with the assumed brammallitic layers of the Arkansas rectorite, the increased number of *cv* sites in the brammallitic layers may be a plausible model. The existence of interstratified *tv*/*cv* mica is also consistent with Al-rich, *cv* 1M illite being more stable than *tv* 1M illite formed during low-temperature diagenesis or hydrothermal conditions (Drits & Zviagina, 2009).

CONCLUSIONS

Rectorite from North Little Rock, Arkansas, occurring as elongated laths, is an interstratification of Na-dominated brammallitic (non-swelling) and beidellitic (swelling) layers, with the structural formula:

$$(Na_{0.53}Mg_{0.03}Ca_{0.03}K_{0.02})$$
$$(Al_{1.96}Fe^{3+}_{0.05}Mg_{0.02})\ [(Si_{3.26}Al_{0.74})\ O_{10}(OH)_2] \quad (8)$$

containing high-charge smectitic layers with a layer charge of 0.48 mol(+)/mol F.U. The calculated CEC value of 64 cmol(+)/kg is slightly higher than measured by the ammonium acetate method, which is typical for high-charge layers (Steudel *et al*., 2009). The dehydroxylation temperature is characterized by a peak doublet in thermal analysis at 470°C and 584°C (±3°C) possibly indicating ≈20% *cis*-vacancies in the octahedral sheets. Although the precise *tv*/*cv* distribution is unknown the high-charge beidellitic layers are assumed to be mainly *tv* and the brammallitic layers have both *tv* and *cv* sites, typical of large octahedral and tetrahedral Al content.

ACKNOWLEDGEMENTS

The authors are grateful to G. Wiederholt and M. Zander from the University of Greifswald for supporting the XRF and TEM measurements, respectively. They thank M. Heinle for ICP-OES measurements and L. Delavernhe from the Karlsruhe Institute of Technology for help with graphical presentation. S. Guggenheim and S. J. Kemp are thanked for their constructive reviews of the manuscript.

REFERENCES

Ahn J.H., Peacor D.R. & Essene E.J. (1985) Coexisting paragonite-phengite in blueshist eclogite: a TEM study. *American Mineralogist,* **70**, 1193–1204.

Anthony J.W., Bideaux R.A., Bladh K.W. & Nichols M. C., editors (1995) Rectorite. *Handbook of Mineralogy*, Mineralogical Society of America, Chantilly, VA 20151-1110, USA. http://www.handbookofmineralogy.org/

Bailey S.W. (1982) Nomenclature for regular interstratifications. *American Mineralogist*, **67**, 394–398.

Barron P.F., Slade P. & Frost R.L. (1985a) Solid-state silicon-29 spin-lattice relaxation in several 2:1 phyllosilicate minerals. *Journal of Physical Chemistry*, **89**, 3305–3310.

Barron P.F., Slade P. & Frost R.L. (1985b) Ordering of aluminum in tetrahedral sites in mixed-layer 2:1 phyllosilicates by solid-state high-resolution NMR. *Journal of Physical Chemistry*, **89**, 3880–3885.

Bishop M.E., Dong H., Kukkadapu R.K., Liu C. & Edelmann R.E. (2011) Bioreduction of Fe-bearing clay minerals and their reactivity toward pertechnetate (Tc-99). *Geochimica et Cosmochimica Acta*, **75**, 5229–5246.

Bradley W.F. (1950) Alternating layer sequence of rectorite. *American Mineralogist*, **35**, 590–595.

Brindley G.W. (1956) Allevardite, a swelling double-layer mica mineral. *American Mineralogist*, **41**, 91–103.

Brown G. & Weir A.H. (1963) The identity of rectorite and allevardite. Pp. 27–35 in: *Proceedings of the International Clay Conference Stockholm 1* (I.T. Rosenqvist & P. Graff-Petersen, editors). Pergamon, Oxford, U.K.

Callière S. & Hénin S. (1950) Sur un nouveau silicate phylliteux: la allevardite. *Comptes Rendus de l'Académie des Sciences*, **230**, 668–669.

Comodi P. & Zanazzi P.F. (1997) Pressure dependence of structural parameters of paragonite. *Physics and Chemistry of Minerals,* **24**, 274–280.

Comodi P. & Zanazzi P.F. (2000) Structural thermal behavior of paragonite and its dehydroxylate: a high-temperature single-crystal study. *Physics and Chemistry of Minerals,* **27**, 377–385.

Drits V.A., Besson G. & Muller F. (1995) An improved model for structural transformations of heat-treated aluminous dioctahedral 2:1 layer silicates. *Clays & Clay Minerals*, **43**, 718–731.

Drits V.A., Lindgreen H., Salyn A.L., Ylagan R. & McCarty D.K. (1998) Semiquantitative determination of *trans*-vacant and *cis*-vacant 2:1 layers in illites and illite-smectites by thermal analysis and X-ray diffraction. *American Mineralogist*, **83**, 1188–1198.

Drits V.A. & Zviagina B.B. (2009) *Trans*-vacant and *cis*-vacant 2:1 layer silicates: Structural features, identification and occurrence. *Clays & Clay Minerals*, **57**, 405–415.

Emmerich K., Wolters F., Kahr G. & Lagaly G. (2009) Clay profiling: The classification of montmorillonites. *Clays & Clay Minerals*, **57**, 104–114.

Emmerich K., Koeniger F., Kaden H. & Thissen P. (2015) Microscopic structure and properties of discrete water layer in Na-exchanged montmorillonite. *Journal of Colloid and Interface Science*, **448**, 24–31.

Gradusov B.P., Chizhikova N.P. & Travnikova L.S. (1968) The nature of interlayer spaces in rectorite from Dagestan. *Doklady Akademii Nauk SSSR, Earth Science Section*, **180**, 130–132.

Guggenheim S., Adams J.M., Bain D.C., Bergaya F., Brigatti M.F., Drits V.A., Formoso M.L.L., Galán E., Kogure T. & Stanjek H. (2006) Summary of recommendations of nomenclature committees relevant to clay mineralogy: report of the Association Internationale pour l'Etude des Argiles (AIPEA) Nomenclature Committee for 2006. *Clay Minerals*, **41**, 863–877.

Inoue A., Kohyama N., Kitagawa R. & Watanabe T. (1987) Chemical and morphological evidence for the conversion of smectite to illite. *Clays & Clay Minerals*, **35**, 111–120.

Inoue A., Velde B., Meunier A. & Touchard G. (1988) Mechanism of illite formation during smectite-to-illite conversion in a hydrothermal system. *American Mineralogist*, **73**, 1325–1334.

Jakobsen H.J., Nielsen N.C. & Lindgreen H. (1995) Sequences of charged sheets in rectorite. *American Mineralogist*, **80**, 247–252.

Kaufhold S., Dohrmann R., Stucki J.W. & Anastácio A.S. (2011) Layer charge density of smectite – closing the gap between the structural formula method and the alkylammonium method. *Clays & Clay Minerals*, **59**, 200–211.

Kitagawa R. (1997) Surface microtopography of rectorite (allevardite) from Allevard, France. *Clay Minerals*, **32**, 89–95.

Klimentidis R.E. & Mackinnon I.D.R. (1986) High resolution imaging of ordered mixed-layer clays. *Clays & Clay Minerals*, **34**, 155–164.

Kodama H. (1966) The nature of the component layers of rectorite. *American Mineralogist*, **51**, 1035–1055.

Kübler B. (1964) Les argiles, indicateurs de métamorphisme. *Revue de L'Institut Francais du Pétrole*, **19**, 1093–1112.

Kübler B. (1967) La cristallinité de l'illite et les zones tout á fait supérieures du métamorphisme. *Étages Tectoniques (Colloque de Neuchatel)*, 105–121.

Lagaly G. & Weiss A. (1971) Neue Methoden zur Charakterisierung und Identifizierung quellungsfähiger Dreischichttonminerale. *Zeitschrift für Pflan zenernährung und Bodenkunde*, **130**, 9–24.

Lantenois S., Muller F., Beny J.-M., Mahiaoui J. & Cham pallier R. (2008) Hydrothermal synthesis of beidellites: characterization and study of the *cis*- and *trans*-vacant character. *Clays & Clay Minerals*, **55**, 39–48.

Mackenzie R.C. (1951) A micromethod for determination of cation-exchange capacity of clay. *Journal of Colloid Science*, **6**, 219–222.

Matsuda T., Kodama H. & Yang A.F. (1997) Ca-rectorite from Sano Mine, Nagano Prefecture, Japan. *Clays & Clay Minerals*, **45**, 773–780.

Meier L.P. & Kahr G. (1999) Determination of the cation exchange capacity (CEC) of clay minerals using the complexes of copper(II) ion with triethylenetetramine and tetraethylenepentamine. *Clays & Clay Minerals*, **47**, 386–388.

Miser H.D. & Milton C. (1964) Quartz, rectorite and cookeite from the Jeffrey Quarry, near North Little Rock, Pulaski County, Arkansas. *Arkansas Geological Commission Bulletin*, **21**, 6–19.

Rieder M., Cavazzini G., D'Yakonov Y.S., Frank-Kamenetskii V.A., Gottardi G., Guggenheim S., Koval P.V., Müller G., Neiva A.M.R., Radoslovich E.W., Robert J.-L., Sassi F.P., Takeda H., Weiss Z. & Wones D. (1998) Nomenclature of micas. *The Canadian Mineralogist*, **36**, 41–48.

Schollenberger C.J. & Dreibelbis F.R. (1930) Analytical methods in base exchange investigations on soils. *Soil Science*, **30**, 161–174.

Smykatz-Kloss W. (1967) Über die Möglichkeit der halbquantitativen Mineralbestimmung mit der DTA ohne Flächenintegration. *Contributions to Mineralalogy and Petrology*, **16**, 481–502.

Środoń J. (2013) Identification and Quantitative Analysis of Clay Minerals. Pp. 25–49 in: *Handbook of Clay Science* (F. Bergaya & G. Lagaly, editors), Elsevier, Amsterdam.

Steudel A. & Emmerich K. (2013) Strategies for the successful preparation of homoionic smectites. *Applied Clay Science*, **75–76**, 13–21.

Steudel A., Weidler P.G., Schuhmann R. & Emmerich K. (2009) Cation exchange reactions of vermiculite with Cu-triethylenetetramine as affected by mechanical and chemical treatment. *Clays & Clay Minerals*, **54**, 486–493.

Stevens R.E. (1946) A system for calculating analyses of micas and related minerals to end members. *United States Geological Survey Bulletin*, **950**, 101–119.

Tsipursky S.I. & Drits V.A. (1984) The distribution of octahedral cations in the 2:1 layers of dioctahedral smectites studied by oblique-texture electron diffraction. *Clay Minerals*, **19**, 177–193.

Wang X., Du Y., Luo J., Lin B. & Kennedy J.F. (2006) Chitosan/organic rectorite nanocomposite films: Structure, characteristic and drug delivery behavior. *Carbohydrate Polymers*, **69**, 41–49.

Wolters F. & Emmerich K. (2007) Thermal reactions of smectites – Relation of dehydroxylation temperature to octahedral structure. *Thermochimica Acta*, **462**, 80–88.

Wolters F., Lagaly G., Kahr G., Nueesch R. & Emmerich K. (2009) A comprehensive characterization of dioctahedral smectites. *Clays & Clay Minerals*, **57**, 115–133.